A Linear *trans*-Bis(imido) Neptunium(V) Actinyl Analog: Np^V(NDipp)$_2$(^{t}Bu$_2$bipy)$_2$Cl (Dipp = 2,6-^{i}Pr$_2$C$_6$H$_3$)

Jessie L. Brown,[†] Enrique R. Batista,*,[‡] James M. Boncella,[†] Andrew J. Gaunt,*,[†] Sean D. Reilly,[†] Brian L. Scott,[§] and Neil C. Tomson[†]

[†]Chemistry, [‡]Theoretical, and [§]Materials Physics and Applications Divisions, Los Alamos National Laboratory, Los Alamos, New Mexico 87545, United States

S *Supporting Information*

ABSTRACT: The discovery that imido analogs of actinyl dioxo cations can be extended beyond uranium into the transuranic elements is presented. Synthesis of the Np(V) complex, Np(NDipp)$_2$(^{t}Bu$_2$bipy)$_2$Cl (**1**), is achieved through treatment of a Np(IV) precursor with a bipyridine coligand and lithium-amide reagent. Complex **1** has been structurally characterized, analyzed by ^{1}H NMR and UV–vis–NIR spectroscopies, and the electronic structure evaluated by DFT calculations.

One of the longest standing debates in actinide chemistry is the extent to which covalent bonding contributions are accessible and the role of the valence 5f/6d orbitals in such metal–ligand interactions.[1,2] The most direct manifestations of covalency are in molecules containing metal–ligand inter-actions with multiple-bond character. The number of examples of uranium–ligand multiple bonds has burgeoned in recent years, with characterizations including nitrides, carbenes, imidos, and terminal chalcogenide functionalities, in addition to other moieties.[3–15] This progress has greatly increased comprehension of uranium electronic structure, bonding, and reactivity. Of particular impact was the discovery that linear *trans*-bis(imido) analogs of the uranyl cation were isolable despite the species proving elusive for many years.[16–18] What has been lacking, however, is an ability to determine how covalency/multiple-bonding changes across the actinide series, and what impact this has on reactivity and redox stability.
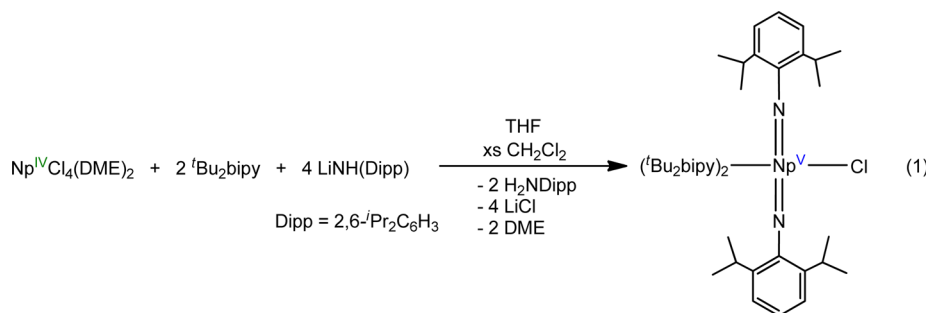
Our previous attempts to synthesize a transuranic bis(imido) molecule through oxidation of plutonium metal, in an analogous fashion to the preparative route for the first U(VI) *trans*-bis(imido), demonstrated differences between U and Pu redox properties with oxidation of Pu^0 beyond Pu(III) not observed.[19] Similar attempts to oxidize Pu(III) species in the pursuit of imido functionalities were also unsuccessful.[19] Although alternative routes to Pu–imido complexes may still be possible, under the reaction conditions explored there was a propensity for trivalent Pu(III) to prevail, a property that impedes formation of imido complexes in oxidation states of IV, V, or VI. Neptunium sits in between uranium and plutonium, increasing the likelihood that it will display intermediate behavior and be more amenable to imido formation in oxidation states higher than III. However, the synthetic protocol for neptunium experiments could not mimic the conditions of the original uranium bis(imido) report,[16]

because there are no readily available sources of Np^0 metal or nonaqueous organic-soluble Np(III) starting materials (the only examples reported were prepared from Np^0 as the precursor).[20] Instead, the recent development of NpCl$_4$(DME)$_2$ (DME = 1,2-dimethoxyethane), as an access point into air/moisture-sensitive Np(IV) chemistry, afforded a first opportunity to explore routes to neptunium-imido species.[21] Herein, we report the successful isolation and characterization of a linear *trans*-bis(imido) Np(V) complex, namely, Np(NDipp)$_2$(^{t}Bu$_2$bipy)$_2$Cl (**1**) (Dipp = 2,6-^{i}Pr$_2$C$_6$H$_3$, ^{t}Bu$_2$bipy = 4,4′-di-*tert*-butyl-2,2′-bipyridyl).

In 2011, it was reported that treatment of UI$_4$(OEt$_2$)$_2$ with 2 equiv of LiNH^{t}Bu and 1 equiv of ^{t}Bu$_2$bipy afforded the U(IV) mono(imido) complex, U(N^{t}Bu)(^{t}Bu$_2$bipy)(THF)$_2$I$_2$.[22] A similar reaction with LiNHDipp, using UCl$_4$ as the precursor, resulted in isolation of a dimeric mono(imido) U(IV) species containing bridging imido groups.[22] Therefore, if imido formation was possible for Np, the initial synthetic product using NpCl$_4$(DME)$_2$ as a precursor was expected to be a Np(IV) mono(imido) complex. Surprisingly, treatment of NpCl$_4$(DME)$_2$ with 1 equiv of ^{t}Bu$_2$bipy and 2 equiv of LiNHDipp resulted in formation of a hexanes soluble fraction (whereas the U(IV) mono(imido) species with the NDipp^{2-} ligand is hexanes insoluble) and isolation of **1**, a Np(V) *trans*-bis(imido) complex, as determined by X-ray crystallography. Interestingly, under slightly different conditions and reagent stoichiometries, a similar oxidation process has been observed for uranium where reaction of UCl$_4$ with 4 equiv of LiNHDipp and 2 equiv of ^{t}Bu$_2$bipy yielded U(NDipp)$_2$(^{t}Bu$_2$bipy)$_2$Cl, a U(V) *trans*-bis(imido) molecule.[17] Therefore, based on the uranium chemistry, we attempted a "rational" synthesis of **1** by treating NpCl$_4$(DME)$_2$ with 2 equiv of ^{t}Bu$_2$bipy and 4 equiv of LiNHDipp. Following extraction into hexanes, single-crystals were obtained in low yield and confirmed by unit cell determination to also be complex **1**. It should be further noted that in the uranium case, halogen atom abstraction from adventitious CH$_2$Cl$_2$ was suspected to be the cause of the oxidation, a proposition that was supported by the observation that deliberate addition of CH$_2$X$_2$ (X = Cl, Br, I) to the reaction resulted in the formation of the corresponding X-halide containing bis(imido) species.[17] Therefore, treating NpCl$_4$(DME)$_2$ with 2 equiv of ^{t}Bu$_2$bipy, 4 equiv of LiNHDipp, and deliberate addition of excess CH$_2$Cl$_2$ results in isolation of

$$Np^{IV}Cl_4(DME)_2 + 2\,^tBu_2bipy + 4\,LiNH(Dipp) \xrightarrow[\substack{-\,2\,H_2NDipp \\ -\,4\,LiCl \\ -\,2\,DME}]{\substack{THF \\ xs\,CH_2Cl_2}} (^tBu_2bipy)_2 \!-\! Np^V \!-\! Cl \quad (1)$$

$$Dipp = 2,6\text{-}^iPr_2C_6H_3$$

1 as dark-red crystals in 17% yield, based on neptunium (eq 1). Although this "bulk product" yield is relatively low, the reaction is reproducible with consistent isolation of the product as single-crystals.

Complex **1** crystallizes in the orthorhombic space group *Pbcn* as **1**·2(H₂NDipp)·O(C₄H₈), with two H₂NDipp molecules and one THF molecule present in the lattice (Figure 1). The
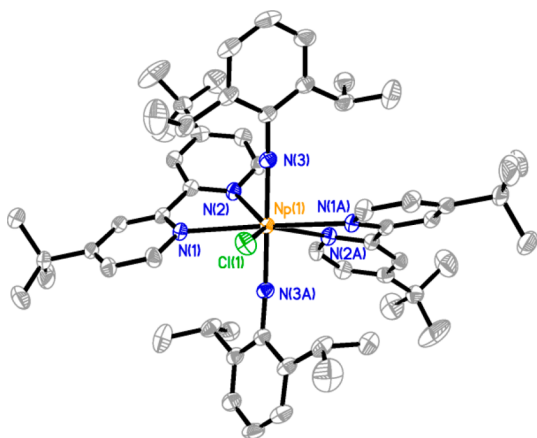

Figure 1. Solid-state molecular structure of Np-(NDipp)₂(^tBu₂bipy)₂Cl, **1**·2(H₂NDipp)·O(C₄H₈), with 50% probability ellipsoids. THF, H₂NDipp, and hydrogen atoms are omitted for clarity. Selected bond lengths (Å) and angles (deg): Np1−N3 = 1.960(3), Np1−N3A = 1.961(3), Np1−N1 = 2.602(3), Np1−N2 = 2.627(3), Np1−Cl1 = 2.7256(12), N3−Np1−N3A = 179.29(17), N3−Np1−Cl1 = 89.64(8), N3A−Np1−Cl1 = 89.65(8).

Np(V) center is seven-coordinate with a distorted pentagonal bipyramidal geometry. The Np−N$_{imido}$ distances (Np1−N3 = 1.960(3) Å and Np1−N3A = 1.961(3) Å) are comparable to the U−N$_{imido}$ distances in the U(V) *trans*-bis(imido) analog (U1−N1 = 1.977(4) and U1−N2 = 1.980(4) Å).[17] For comparison, the only example of the amide version of the NHDipp$^{1−}$ ligand coordinated to an actinide is the U(III) compound [K(THF)₂]₂[U(NHDipp)₅], in which the U−N distances are much longer with an average value of 2.34 Å.[23] The linearity of the bis(imido) fragment in **1** is reflected by an N3−Np1−N3A bond angle of 179.29(17)°. The Np−Cl distance of 2.7256(12) Å is also consistent with assignment as a Np(V) species, again comparable to the U(V) analog U−Cl distance of 2.729(2) Å.[17] The C−C bond length of 1.485(6) Å in the bipyridine ligands is as expected for the neutral ligand, and there is no indication of ligand reduction to radical anions which would significantly shorten the C−C bridge distance. Lastly, the N−C bond distance of 1.398(6) Å in the uncoordinated lattice aniline molecule is more consistent with what has been observed before for free lattice Dipp-aniline not

the Dipp-anilinium cation which has a N−C bond distance of the order of 1.47 Å.[24,25]

Complex **1** is soluble in hexanes, toluene, and ethereal solvents. The room temperature ¹H NMR spectrum of **1** in C₆D₆ exhibits a number of paramagnetically broadened and shifted resonances consistent with a Np(V) center. Specifically, the protons of the bipyridyls' ^tBu substituents are observed at −5.8 and −6.6 ppm, while the ^iPr protons of the imido ligands are observed at 12.6 ppm (see Supporting Information, SI). Consistent with the solid-state molecular structure of **1**, 2 equiv of free aniline are observed in the ¹H NMR spectra and are readily assignable. Several attempts were made to optimize the isolated yield of **1**, and the SI provides greater discussion of ¹H NMR spectroscopic studies, reaction progression, and stability of **1** under various conditions. Complex **1** was further characterized by UV−vis−NIR spectroscopy. The UV−vis−NIR spectrum of **1** in toluene is dominated by charge-transfer transitions that extend beyond 800 nm (Figure 2, red
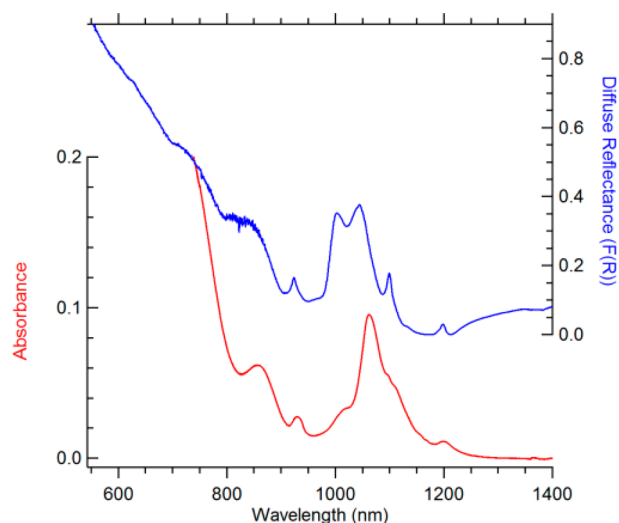

Figure 2. UV−vis−NIR diffuse reflectance spectrum of solid Np(NDipp)₂(^tBu₂bipy)₂Cl (**1**) (blue spectrum, right axis) and the solution spectrum of the dissolved solid in toluene (red spectrum, left axis) for comparison. Only the vis−NIR region of the spectra are shown here.

spectrum). Several transitions observed in the 800−1200 nm region seem to originate from Np 5f to N$_{imido}$ 2p transitions, as discussed in the section below. In the solid-state (Figure 2, blue spectrum), ground crystals of **1** exhibit broadly similar electronic absorptions as the solution-phase, with some minor shifts in the band energies and relative intensities, as has been previously noted in solid versus solution comparisons of molecular Pu compounds.[26] The phase differences could

possibly be accounted for by changes in the local symmetry/coordination geometry of the ligands about the Np(V) center in solution versus the solid state. Alternatively, orientation dependence of the electronic absorption spectra of single-crystals of neptunium compounds has previously been documented,[27] with crystal rotation resulting in enhancement and/or reduction in intensity of certain transitions. The solid-state spectrum of **1** was measured on ground-up crystalline samples, meaning that the effect of axis orientation was not probed, but the possibility of some solid-state versus solution-phase differences arising from this phenomenon cannot be discounted.

Since complex **1** is the first example of a transuranic imido group (and the first molecular Np−ligand multiple-bond beyond dioxo neptunyl cations), electronic structure details were probed by density functional theory (DFT) calculations and compared to the U(V) analog synthesized by Boncella et al.,[17] but not previously analyzed by DFT. For the sake of computational speed and to ease the convergence of the optimizations, the equatorial $^tBu_2$bipy ligands in **1** were replaced by 2,2′-bipyridyl (avoiding the ^tBu substituents), and the isopropyl substituents (of the axial imido (NDipp)$^{2-}$ ligands) were replaced by methyl groups (see SI). Similarly, the U(V) analog was computed with the same set of ligands to make the comparison more appropriate. The optimized structures of these model systems are in close resemblance to those of the experimentally determined structures. For example, the average Np−N$_{(imido)}$ bond distance (1.966 Å, 0.3% difference) and the Np−Cl bond distance (2.742 Å, 0.6% difference) match well with the solid-state molecular structure of **1**. Lastly, the uranium model has a U−N bond distance of 1.978 Å (exp. U−N$_{av.}$ = 1.979 Å, 0.2% difference) which also matches closely to the solid-state structure found experimentally.[17] The electronic state of the Np(V) complex is a triplet f^2 system, with two unpaired electrons in (f_δ, f_φ) orbitals. The U(V) analog is a doublet f^1 system with unpaired spin density in f_δ (see SI).

We also attempted to identify the theoretical Np−N and U−N vibrational modes. However, the vibration of the An−N bond is not a normal mode of the molecule due to its strong coupling to the rest of the imido ligand. Specifically, the vibrational modes of the C−C bonds couple with the C−N bond, leading to coupling between the Np−N bond and the rest of the ligand. This is also observed in the simulated vibrational modes of the uranium(V) analog. In order to obtain a quantification of this coupling the asymmetric displacement of the N−An−N unit was projected over the normal modes of each molecule. The largest overlap between the asymmetric displacement for the Np complex was with the mode at 945 cm^{-1} and for the U complex the main contribution was from two modes at 944 and 943 cm^{-1} (peaks are observed in the experimental Raman spectra at 899 cm^{-1} for the Np(V) complex **1** and at 908 cm^{-1} for the U(V) analog). All these modes are Raman intensive, however they represent <40% of the asymmetric displacement, hence making it difficult to correlate a shift in the frequency with a difference in the bond strength. The remaining 60% of the asymmetric displacement converges very slowly needing at least an expansion over 10 modes to describe the second 40% (see SI). This analysis serves as evidence of the difficulty in interpreting infrared and Raman spectroscopy in actinide bis(imido) complexes. This contrasts with bis(oxo) analogs, which due to the terminal nature of the O^{2-} anions, the symmetric and asymmetric stretches are key

signatures in the spectrum that relate to the strength of the bonding in the linear actinyl moiety.

Time-dependent DFT was also used to interpret the Np UV−vis−NIR spectra shown in Figure 2. The excited states are a combination of multiple transitions from occupied to virtual orbitals. The natural transition orbitals analysis gives a clean particle-hole picture with the excited electrons in the antibonding orbitals of Np(5f) and N(2p) orbitals (Figure 3). Excitations 1 and 2 are pure 5f to 5f transitions. Excitation 3
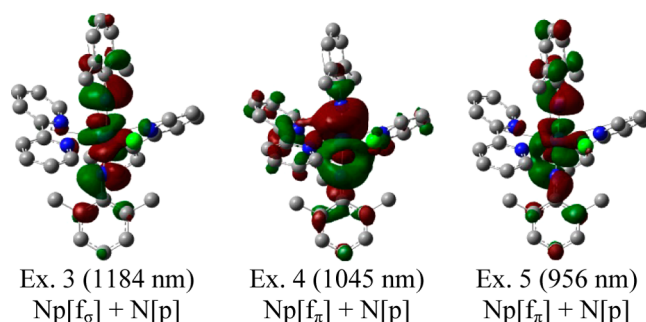

Ex. 3 (1184 nm)   Ex. 4 (1045 nm)   Ex. 5 (956 nm)
Np[f_σ] + N[p]   Np[f_π] + N[p]   Np[f_π] + N[p]

Figure 3. Particle orbitals for the calculated excited states from the singly occupied Np(5f) into the antibonding Np(5f)−N(2p) orbitals. These transitions yield the intensity observed in the 1200−950 cm^{-1} region of the UV−vis−NIR spectrum.

is into the Np(5f$_\sigma$)−N(2p) antibonding, and excitations 4 and 5 are into the Np(5f$_\pi$)−Np(2p) antibonding orbitals. The six excitations of the two f electrons into the Np(5f)−N(2p) antibonding orbitals are identified in the range between 1200 and 960 nm (Figure 3), in clear correspondence with the transitions shown in the experimental spectrum. The analogous excitations for the uranium compound are higher in energy, mixed among the metal-to-ligand excitations (see SI). The virtual U−N orbitals being higher in energy than the virtual Np−N orbitals is also indicative of stronger bonding in the uranium compound with more stabilized bonding orbitals, and hence, more destabilized virtual orbitals. Because the Kohn−Sham orbitals show a high degree of mixing between the N−An−N center and the ligand, effectively spreading the An(d) and An(f) populations over many molecular orbitals, we turned to the natural bond orbital (NBO) analysis to obtain a cleaner picture. The NBO results are consistent with the excitation spectrum predicting the bonding orbitals to be more stabilized in the U complex, and correspondingly, the antibonding orbitals are destabilized in comparison with the Np complex. The energy of the U−N antibonding NBOs (3.14 eV) is on average 0.91 eV higher than the Np−N antibonding NBOs (2.23 eV), whereas the bonding NBOs of U (−5.83 eV) are 0.05 eV more stable than the corresponding Np orbitals (−5.78 eV), yielding the higher excitation energy of 950 cm^{-1} and above for U(5f) into antibonding U(5f)−N(2p) orbitals. The bonding orbitals from the NBO analysis are 30%Np−70%N hybridizations with both Np(6d) and Np(5f) orbitals participating in a 40%−60% split. In the uranium complex the metal participation in the NBO bonding orbitals is 24% (76% being N(p)) where the U(6d) orbitals contribute 45% of the U participation, the rest being U(5f). The larger degree of metal orbital mixing in **1**, despite the contraction of the actinide orbitals as the series progresses from U to Np, is attributed to the dropping in orbital energies for Np which leads to an improved orbital energy matching between the actinide metal and the imido ligand (see SI).

In conclusion, we have reported the synthesis and isolation of an unprecedented transuranic linear *trans*-bis(imido) moiety, present in Np(NDipp)$_2$(^{t}Bu$_2$bipy)$_2$Cl (**1**), which was structurally characterized. Molecule **1** is a Np(V) complex generated from a Np(IV) precursor by the addition LiNHDipp amide in the presence of bipyridyl coligands. Oxidation to Np(V) is likely facilitated by halide abstraction from CH$_2$Cl$_2$, similar to what has been observed in uranium chemistry. However, **1** was first isolated from reaction conditions and reagent stoichiometries that afford mono(imido) products in uranium chemistry. The difference in reactivity between U(IV) and Np(IV) is important as it highlights the need to study each relevant actinide element in its own right and not rely on surrogates. In general, Np(V) is more stable than U(V), and this could be a reason for the observed oxidation of Np(IV) to Np(V) under conditions that were anticipated to afford Np(IV) mono-(imido) products. The U(V) bis(imido) analog of **1** is only formed under conditions of higher reactant stoichiometry, whereas **1** is isolated under both low and high metal:ligand reagent stoichiometric ratios, consistent with a greater driving force for formation of Np(V) versus U(V). Theoretical calculations verify that the 5f and 6d orbitals of Np(V) are able to engage in significant covalent overlap with the nitrogen 2p orbitals to result in the multiply-bonded [DippN=Np^V=NDipp]$^+$ moiety. This verifies **1** as the first example of a transuranic metal–ligand multiple-bond beyond the ubiquitous actinyl dioxo moiety. Comparing analogous models of the U(V) and Np(V) bis(imido) molecules, the picture is broadly similar for both actinides with significant levels of metal-based orbital participation in the An–N$_{imido}$ bonds. However, the slight enhancement of Np versus U metal orbital mixing in the bonding is explained by the better energy match of the neptunium-based valence orbitals with the imido-based orbitals. Further work is underway to optimize the yield of **1** to allow exploration of subsequent reactivity and electrochemical properties, along with assessing the generality of imido formation with other parent amido ligands and coligands.

■ ASSOCIATED CONTENT

Ⓢ Supporting Information

The Supporting Information is available free of charge on the ACS Publications website at DOI: 10.1021/jacs.5b06667.

> X-ray crystallographic details of **1**. (CIF)
> Complete details of the preparation and characterization of **1**, supplementary NMR reactivity studies, and additional computational details. (PDF)

■ AUTHOR INFORMATION

Corresponding Authors
*erb@lanl.gov
*gaunt@lanl.gov

Notes

The authors declare no competing financial interest.

■ ACKNOWLEDGMENTS

■ REFERENCES

(1) Jones, M. B.; Gaunt, A. J.; Gordon, J. C.; Kaltsoyannis, N.; Neu, M. P.; Scott, B. L. *Chem. Sci.* **2013**, *4*, 1189.
(2) Neidig, M. L.; Clark, D. L.; Martin, R. L. *Coord. Chem. Rev.* **2013**, *257*, 394.
(3) Anderson, N. H.; Odoh, S. O.; Yao, Y.; Williams, U. J.; Schaefer, B. A.; Kiernicki, J. J.; Lewis, A. J.; Goshert, M. D.; Fanwick, P. E.; Schelter, E. J.; Walensky, J. R.; Gagliardi, L.; Bart, S. C. *Nat. Chem.* **2014**, *6*, 919.
(4) Hayton, T. W. *Dalton Trans.* **2010**, *39*, 1145.
(5) Hayton, T. W. *Chem. Commun.* **2013**, *49*, 2956.
(6) Jones, M. B.; Gaunt, A. J. *Chem. Rev.* **2013**, *113*, 1137.
(7) King, D. M.; Liddle, S. T. *Coord. Chem. Rev.* **2014**, *266–267*, 2.
(8) Liddle, S. T. *Angew. Chem., Int. Ed.* **2015**, *54*, 8604.
(9) Gardner, B. M.; Balázs, G.; Scheer, M.; Tuna, F.; McInnes, E. J. L.; McMaster, J.; Lewis, W.; Blake, A. J.; Liddle, S. T. *Angew. Chem., Int. Ed.* **2014**, *53*, 4484.
(10) Gardner, B. M.; Balázs, G.; Scheer, M.; Tuna, F.; McInnes, E. J. L.; McMaster, J.; Lewis, W.; Blake, A. J.; Liddle, S. T. *Nat. Chem.* **2015**, *7*, 582.
(11) Brown, J. L.; Fortier, S.; Wu, G.; Kaltsoyannis, N.; Hayton, T. W. *J. Am. Chem. Soc.* **2013**, *135*, 5352.
(12) Camp, C.; Pécaut, J.; Mazzanti, M. *J. Am. Chem. Soc.* **2013**, *135*, 12101.
(13) Ephritikhine, M. *Organometallics* **2013**, *32*, 2464.
(14) Fox, A. R.; Arnold, P. L.; Cummins, C. C. *J. Am. Chem. Soc.* **2010**, *132*, 3250.
(15) Lu, E.; Cooper, O. J.; McMaster, J.; Tuna, F.; McInnes, E. J. L.; Lewis, W.; Blake, A. J.; Liddle, S. T. *Angew. Chem., Int. Ed.* **2014**, *53*, 6696.
(16) Hayton, T. W.; Boncella, J. M.; Scott, B. L.; Palmer, P. D.; Batista, E. R.; Hay, P. J. *Science* **2005**, *310*, 1941.
(17) Jilek, R. E.; Spencer, L. P.; Lewis, R. A.; Scott, B. L.; Hayton, T. W.; Boncella, J. M. *J. Am. Chem. Soc.* **2012**, *134*, 9876.
(18) Spencer, L. P.; Schelter, E. J.; Yang, P.; Gdula, R. L.; Scott, B. L.; Thompson, J. D.; Kiplinger, J. L.; Batista, E. R.; Boncella, J. M. *Angew. Chem., Int. Ed.* **2009**, *48*, 3795.
(19) Gaunt, A. J.; Reilly, S. D.; Enriquez, A. E.; Hayton, T. W.; Boncella, J. M.; Scott, B. L.; Neu, M. P. *Inorg. Chem.* **2008**, *47*, 8412.
(20) Avens, L. R.; Bott, S. G.; Clark, D. L.; Sattelberger, A. P.; Watkin, J. G.; Zwick, B. D. *Inorg. Chem.* **1994**, *33*, 2248.
(21) Reilly, S. D.; Brown, J. L.; Scott, B. L.; Gaunt, A. J. *Dalton Trans.* **2014**, *43*, 1498.
(22) Jilek, R. E.; Spencer, L. P.; Kuiper, D. L.; Scott, B. L.; Williams, U. J.; Kikkawa, J. M.; Schelter, E. J.; Boncella, J. M. *Inorg. Chem.* **2011**, *50*, 4235.
(23) Nelson, J. E.; Clark, D. L.; Burns, C. J.; Sattelberger, A. P. *Inorg. Chem.* **1992**, *31*, 1973.
(24) Bond, A. D.; Doyle, E. L. *Chem. Commun.* **2003**, 2324.
(25) Samas, B.; Macikenas, D. *Acta Crystallogr., Sect. E: Struct. Rep. Online* **2006**, *62*, o2809.
(26) Reilly, S. D.; Scott, B. L.; Gaunt, A. J. *Inorg. Chem.* **2012**, *51*, 9165.
(27) Wang, S.; Alekseev, E. V.; Depmeier, W.; Albrecht-Schmitt, T. E. *Chem. Commun.* **2010**, *46*, 3955.